Scientific Research Publishing

World Journal of Engineering and Technology, 2023, 11, 793-806
https://www.scirp.org/journal/wjet
ISSN Online: 2331-4249
ISSN Print: 2331-4222

Design Optimization for Generating a High Static Magnetic Field

Hussien A. Elharati[1], Salma Ahmed Alharati[2], Ziad Omar Wareg[3], Mohamed Amro Waregh[3]

[1]Department of Electrical Engineering, Higher Institute of Science and Technology, Tripoli, Libya
[2]Physics Department, Ministry of Education, Tripoli, Libya
[3]Higher Institute of Science and Technology, Nalut, Libya
Email: elharati@gmail.com, adawahb.1973@gmail.com, zwrrag2012@gmail.com, mwaregh2009@my.fit.edu

How to cite this paper: Elharati, H.A., Alharati, S.A., Wareg, Z.O. and Waregh, M.A. (2023) Design Optimization for Generating a High Static Magnetic Field. *World Journal of Engineering and Technology*, **11**, 793-806.
https://doi.org/10.4236/wjet.2023.114054

Received: September 6, 2023
Accepted: November 13, 2023
Published: November 16, 2023

Abstract

This paper details the creation of a device capable of generating a powerful and consistent static magnetic field. This apparatus serves the purpose of quantifying the magnetostrictive strain found in materials like annealed cobalt ferrite and Terfenol-D, specifically those shaped as cylindrical rods. In our investigation, the use of static magnetic fields proves most advantageous. This choice is made to mitigate the generation of eddy currents, which would inevitably occur if the magnetic field intensity were varied. The fundamental idea behind this design involves employing a C-shaped iron core constructed from low-carbon mild steel. On this core, three coils are mounted, each capable of producing one-third of the required 9000 Oersted (Oe) magnetic field strength. The test specimen is situated within the "jaws" of the C-shaped core, thus completing the magnetic circuit. To manage the heat generated by each coil, a cooling system consisting of copper tubes is employed. These tubes facilitate the flow of air to dissipate the heat. To model and predict the magnetic field strength produced by the coils, finite element analysis (FEMM) software is utilized, and the results align closely with the anticipated outcomes. This design effectively generates a robust and unchanging magnetic field measuring a stable 9000 Oe in total. Consequently, this equipment finds utility in characterizing the magnetic properties of specific materials.

Keywords

Static Magnetic Field, Magnetostrictive Strain, Eddy Currents, Magnetic Field Strength, Finite Element Method Magnetics (FEMM)

1. Introduction

Intense magnetic fields hold significant importance across various industrial

sectors. These high magnetic fields can be produced through diverse methods, including electromagnets with iron-core or air-core solenoids, superconducting magnets, and pulsed magnets. In some applications, the important requirements are the power available and the field magnitude.

The inception of iron-core electromagnets can be attributed to Sturgeon [1], who demonstrated this innovation by coiling a conductor around a horseshoe-shaped iron bar and passing an electrical current through the winding. In contemporary designs, iron-core electromagnets have the capability to generate static magnetic field strengths of up to 20,000 Oersted (Oe). The magnetic circuit primarily comprises a yoke and two high-permeability, low-carbon steel components. Coils, wound with thousands of turns, encircle the iron cores. The useful magnetic field emanates from the air gap, and its strength is significantly influenced by the current supplied to the coils, the permeability of the iron core, and the physical dimensions of the magnetic circuit—particularly the air gap distance and core length. To prevent damage to the insulating material around the copper wire, the coils are cooled either by water or air. Key electromagnet specifications encompass the maximum magnetic field produced in the air gap, power consumption, maximum current capacity, and the requisite cooling, whether through water or air.

Air-core solenoids demand higher power inputs when aiming to generate intense magnetic fields at their centers compared to iron-core solenoids. One of the initial designs for air-core magnets was executed by Montgomery [1], resulting in the generation of 250,000 gauss while consuming 12 megawatts of power. This system comprised three coaxial solenoids and utilized a water-cooling system with a flow rate of 3000 gallons per minute to dissipate heat generated in each coil. More recently, Rafferty *et al.* [2] described an air-core design tailored for measuring the magnetostrictive strain of materials like Terfenol-D, using a copper solenoid to create a static magnetic field with a maximum strength of 750 Oe.

Present-day electromagnets available in the market are capable of producing magnetic field strengths ranging from 25,000 to 30,000 Oe. The maximum field achievable hinges on the maximum current capacity, which is constrained by the insulating properties of the copper wire used. To augment current capacity without damaging the insulation layer, an effective cooling system must be employed to dissipate the heat generated in the coils.

In the range of 100,000 to 400,000 Oe, pulsed magnets are employed to generate magnetic fields. Employing this approach, Jana *et al.* [3] applied a 2.5 kV direct current voltage through a capacitor bank to produce a magnetic field of nearly 8 Tesla (T).

Superconducting magnets consist of solenoids composed of superconducting coils, utilizing wires made of type II superconductors such as niobium titanium. These wires are maintained at liquid helium temperatures, and the solenoid itself must be immersed in a liquid helium bath. Superconducting magnets can sustain very high current densities with minimal resistance and require little to no elec-

trical power input. Ozaki *et al.* [4] designed a superconducting magnet using Nb3Sn and NbTi conductors, achieving a central magnetic field strength of 17 T. Cryogen-free superconducting magnets (CFM) are built upon Gifford-McMahon refrigeration technology and do not rely on liquid helium for cooling. This cryogen-free approach marks a significant breakthrough, given the expense and difficulty associated with obtaining liquid helium. Today, numerous cryogen-free magnets are operational worldwide, with the capacity to produce magnetic fields in the range of 18 to 20 Tesla (T).

Another method for generating high magnetic fields involves the use of a vibrating sample magnetometer (VSM). VSMs typically comprise an electromagnet, a mechanism to vibrate the sample within a magnetic field environment, and detection coils that generate a signal voltage in response to changes in flux emanating from the vibrating sample. Lo *et al.* [5] successfully employed a VSM to generate a static magnetic field of 4000 Oersted (Oe), employing this technique to magnetically anneal cobalt ferrite ceramics.

The primary objective of the apparatus presented here is to generate a robust and steady magnetic field reaching up to 9000 Oe. This magnetic field is crucial for conducting magneto strictive strain tests on materials with magneto strictive properties. In the case of cobalt ferrite, it enables the measurement of saturation magnetostriction. Additionally, this field is suitable for annealing cobalt ferrite samples, a process previously demonstrated by Bozorth *et al.* [6] to significantly enhance cobalt ferrite's magnetostriction.

For this specific investigation into magnetic properties, the generation of a static magnetic field is preferred. The use of non-static magnetic fields can introduce various electromagnetic effects, complicating the analysis of the system and leading to energy losses due to eddy currents.

2. Apparatus

2.1. Iron-Core Coil

When an electric current, denoted as I, flows through a conductor, it generates a magnetic field surrounding the conductor [7]. To produce a strong and focused magnetic field, one can create a coil comprising N turns of wire. This coil is fashioned by winding the conductor around an iron core or a coil spool. The magnetic field's strength is directly linked to both the number of turns and the current passing through the coil. As the current traverses the coil, the magnetic field around each wire turn interacts with the fields produced by adjacent turns. The cumulative effect of all these turns' results in a two-pole field similar to that of a basic bar magnet, where one end of the coil acts as a south pole, and the opposite end serves as a north pole.

The efficiency of generating a magnetic field can increase significantly, by a factor of a thousand, when the coil is wound around an iron core. In this context, the core is composed of iron, which is known for guiding a magnetic flux along a circuit, much like how a copper conductor conducts electric current along a circuit [8].

2.2. C-Shape Design

The fundamental idea behind the design revolves around the utilization of a C-shaped core crafted from low-carbon mild steel with a circular cross-section measuring 30 mm in diameter. When conducting tests, the designated sample is positioned within the "jaws" of this C-shaped core, effectively completing the magnetic circuit. Figure 1 provides a visual representation of the construction of this C-shaped coil. The sample itself has a length of 50 mm, and there are 1 mm-wide air gaps on either side. It is anticipated that upon the generation of the magnetic field, the sample will move, making contact with one of the "jaws" of the C-shaped core, resulting in a 2 mm-wide air gap on one side of the sample.

To achieve a specific magnetic flux density B within the air gap, a certain number of ampere-turns (N) are necessary in the coil winding. Additionally, determining the required current for the system is a crucial aspect. These parameters can be calculated using Equation (6). As indicated in Table 1, a greater number of turns results in a reduced current requirement. Likewise, a shorter core length corresponds to a lower current requirement.

The most energy-efficient approach to reach the desired 9000 Oersted (Oe) magnetic field involves employing 24,000 turns and a core length of 3.828 meters.

To avoid the complexity of continuously winding 24,000 turns around the iron core, a more practical approach is to create three separate coils, each consisting of 8000 turns. These windings are organized into 10 layers, with each layer containing 800 turns. The coils are constructed using polyurethane-coated copper wire, and you can find the specifications of this wire in Table 2. The winding process is conducted using a standard workshop lathe.

2.3. Air-Gap Considerations

During the magneto strictive strain testing and magnetic annealing processes, a cobalt ferrite sample is positioned within the space between the "jaws" of the C-shaped core. Consequently, the magnetic properties of the cobalt ferrite sample play a significant role in determining the resulting magnetic field strength within the "jaws" of the C-shaped core.

As an initial assumption, it is presumed that the magnetic flux within the iron core possesses the same value as the flux within the air gap and the sample. This assumption implies that there is no flux leakage. Therefore, when both the sample and the iron core share the same diameter, the flux density is also assumed to be identical. If the air gap is substantially narrower in comparison to this diameter, the flux density (denoted as B) in the air gap is approximately equivalent as well. However, it's crucial to note that the magnetic field strengths within the air gap and the iron core differ significantly. These differences are attributed to the energy required to establish the magnetic flux, with iron requiring significantly less energy than air. This principle is governed by the circuital law of magnetism [8].

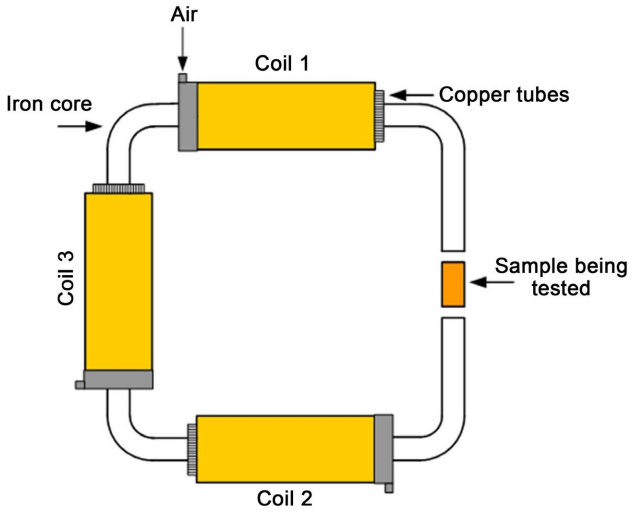

Figure 1. Construction of the "C-shaped" coil design.

Table 1. Calculation of number of turns and current required by the system.

Length of iron core (m)	N (turns)	$N \times I$ (ampere-turn)	Current (amps)
1	9000	42755.6	4.751
	15,000	42755.6	2.850
	18,000	42755.6	2.375
	24,000	42755.6	1.781
2	9000	47055.6	5.228
	15,000	47055.6	3.137
	18,000	47055.6	2.614
	24,000	47055.6	1.961
3	9000	51355.6	5.706
	15,000	51355.6	3.424
	18,000	51355.6	2.853
	24,000	51355.6	2.140
4	9000	54,916	6.102
	15,000	54,916	3.661
	18,000	54,916	3.051
	24,000	54,916	2.288

Table 2. Specification of the enamelled copper wire.

Resistivity	SWG	Diameter (mm)	Diameter including insulation (mm)	Temperature handling
1.68×10^{-6}	22	0.71	0.776	200˚C

$$N \times I = \oint Hdl \tag{1}$$

where N is the number of turns in the coil, I is the current, H is the magnetic field strength and l is the length of each component in the circuit. Splitting the circuit into its component parts:

$$N \times I = \oint Hdl = \left(H_c \times l_c\right) + \left(H_g \times l_g\right) + \left(H_s \times l_s\right) \tag{2}$$

where the subscripts *c*, *g* and *s* refer to the iron core, the air gap and the sample being tested, respectively. But by definition

$$H_c = \frac{B}{\mu_{r_c} \times \mu_o} \tag{3}$$

$$H_g = \frac{B}{\mu_o \times \mu_{r_g}} \tag{4}$$

$$H_s = \frac{B}{\mu_{r_s} \times \mu_o} \tag{5}$$

where:

$B =$ Magnetic flux density.

μ_r is the relative permeability.

$\mu_{r_g} =$ Relative permeability of air in the gap, assumed to be equal to 1.

$\mu_o =$ Permeability of free space = $4\pi \times 10^{-7}$.

If flux leakage is neglected, B will be constant. It follows that:

$$N \times I = \frac{B}{\mu_o}\left[\left(\frac{l_c}{\mu_{r_c}}\right) + l_g + \left(\frac{l_s}{\mu_{r_s}}\right)\right] \tag{6}$$

In the development of the test system, a critical requirement is that the sample under examination, measuring 50 mm in length and 30 mm in diameter, should be subjected to a magnetic field strength of 9000 Oersted (Oe), which is equivalent to 716,000 A/m. However, to proceed with the design, it is imperative to possess knowledge of the magnetic properties of the cobalt ferrite sample under this magnetic field strength. Ideally, these properties should be determined through experimental measurements.

If it is possible to measure the flux density, denoted as B, within the sample when a magnetic field strength of 9000 Oe is generated, we can establish a specific value for B. The relative permeability of the sample material can be estimated using the following formula:

$$\mu_{r_s} = \frac{B}{H_s \mu_o} \tag{7}$$

Once the flux density, *B*, has been estimated, the experimental data also can be used to provide an estimate for the relative permeability of the specific iron alloy. This gives a value for μ_{r_c}. Values are thus available to complete the right-hand side of Equation (6), since lc = 3.828 m, ls = 0.05 m and lg = 0.002 m. Input of these geometric values therefore allows an estimate for the left-hand side of Equation (6), to be arrived at, where $N \times I$ is the product of the current and the

number of turns in the coil. The total number of turns has already been established at 24,000, and so I can be estimated. This calculation, however, is not complete until the power requirements of the system have been estimated, and this depends on the value of the total resistance of the copper wire in the coils which is carried out in Section 2.4.

In an attempt to estimate a value for the flux density, *B*, of cobalt ferrite, values have been extrapolated from unpublished data generated in a previous project. From this extrapolation, it emerged that the flux density in the sample must reach a value of 1.662221 T when the magnetic field strength is 9000 Oe. This value was used to calculate estimates for the permeability and relative permeability given in Table 3.

Given that these values are derived from extrapolated data rather than actual experimental results, they introduce a degree of uncertainty into the design process. The true validation of the system's ability to meet the design criteria, specifying certain conditions, can only be established by physically constructing the equipment and conducting measurements of the magnetic properties. However, it was anticipated that the design would have the flexibility to adjust the factors influencing the magnetic field strength, such as increasing or decreasing the current in the coil. Consequently, it was expected that the equipment could be modified to achieve the desired design requirements.

By employing the flux density value, *B*, the magnetic field strength within the air gap can be calculated as follows:

$$H_g = \frac{B}{\mu_o} = \frac{1.662221}{4\pi \times 10^{-7}} = 1322.7534 \text{ kA/m} \tag{8}$$

From the literature (1020 low carbon steel B-H data), the magnetic field strength required to produce a flux density of 1.662221 T in the iron core is about 4300 A/m [9]. This gives the permeability of the iron to be:

$$\mu_c = \frac{B}{H} = \frac{1.662221}{4300} = 0.000387 \text{ Tm/A} \tag{9}$$

It follows that the permeability of the iron core is:

$$\mu_{r_c} = \frac{\mu_c}{\mu_0} = \frac{0.000387}{4\pi \times 10^{-7}} = 307.6171 \tag{10}$$

Using Equation (6), the current required to activate each layer in each coil can be calculated as follows:

$$N \times I = H_g \left(\frac{l_c}{\mu_{r_c}} + l_g + \frac{l_s}{\mu_{r_s}} \right) = 1322.7534 \times 1000 \left(\frac{3.828}{307.6171} + 0.002 + \frac{0.05}{1.8469} \right)$$

$N \times I =$ 54,916 Ampere-turn, but N = 24,000, then $I =$ 2.2882 Amps.

2.4. Estimation of Electrical Resistance of Copper Wire of Each Coil

In each coil, the resistance of each layer can be calculated using this formulae:

Table 3. Magnetic properties of cobalt ferrite at 9000 Oe.

Magnetic field density (B)	Permeability (μ_s)	Relative permeability (μ_{rs})
1.6622 T	2.3209×10^{-6} Tm/A	1.8469

$$R = \frac{\rho \times l}{A} \tag{11}$$

where:

ρ The resistivity, l the length of wire in each layer, and A is the cross-sectional area of copper wire.

Table 4 shows and describes the length of wire in each layer and the resistances in each layer at room temperature. The total length of wire needed to form one coil was about 1326 meters.

To estimate the total resistance of each coil, layers in each coil can be connected either in series, in parallel or in a combination of both, a semi series/semi parallel arrangement.

2.4.1. Series Connection

If the 10 layers in each coil are connected in series, then the total resistance would be given by:

$$R_T = R_{l_1} + R_{l_2} + R_{l_3} + R_{l_4} + R_{l_5} + R_{l_6} + R_{l_7} + R_{l_8} + R_{l_9} + R_{l_{10}} \tag{12}$$

The total resistance in each coil would be about 56.266 Ω, and the potential difference across the coil would be about 129.4 V if, for instance, the current was 2.3 Amps. If the three coils are connected in series the total potential difference would be 388.2 volts.

2.4.2. Semi Series/Semi Parallel Arrangement

To simplify calculations, it is necessary to ensure that each layer in each coil will receive the same amount of current (2.2882 Amps). The arrangement shown in **Figure 2** fulfils this requirement. The total resistance of each coil would be given by:

$$\frac{1}{R_{total}} = \frac{1}{R_{l_1}} + \frac{1}{R_{l_{10}}} = \frac{1}{R_{l_2}} + \frac{1}{R_{l_9}} = \frac{1}{R_{l_3}} + \frac{1}{R_{l_8}} = \frac{1}{R_{l_4}} + \frac{1}{R_{l_7}} = \frac{1}{R_{l_5}} + \frac{1}{R_{l_6}} \tag{13}$$

Table 5 reveals the total resistance of each coil when the resistivity of copper is calculated at 20˚C and 150˚C.

Series connection arrangement was ruled out in favor of semi-series/semi-parallel, as the latter arrangement gives a lower potential difference across the coils. Based on the current value calculated in Section 2.3, values of voltage and power consumed by the system can be calculated. **Table 6** shows the results, the data emphasize that the rig is therefore a success in terms of length, coil winding, current, voltage, and power.

The resistances of each layer of each coil were measured at room temperature using a digital multimeter (Tektronix DMM 912) and showed reasonable agreement with the calculated theoretical values as shown in **Figure 3**. Measured

Table 4. Length of copper wire of each layer in one coil at room temperature.

Layer no.	Radius (m)	Circum. (m)	Length of 800 turns	R of each layer when ρ @ 20˚C
1	0.0154	0.0967	77.3485	3.2821
2	0.0192	0.1204	96.3288	4.0875
3	0.0199	0.1253	100.2294	4.2530
4	0.0237	0.1490	119.2096	5.0584
5	0.0245	0.1539	123.1102	5.2239
6	0.0283	0.1777	142.0905	6.0293
7	0.0290	0.1825	145.9911	6.1948
8	0.0328	0.2062	164.9713	7.0002
9	0.0336	0.2111	168.8719	7.1657
10	0.0374	0.2348	187.8522	7.9711

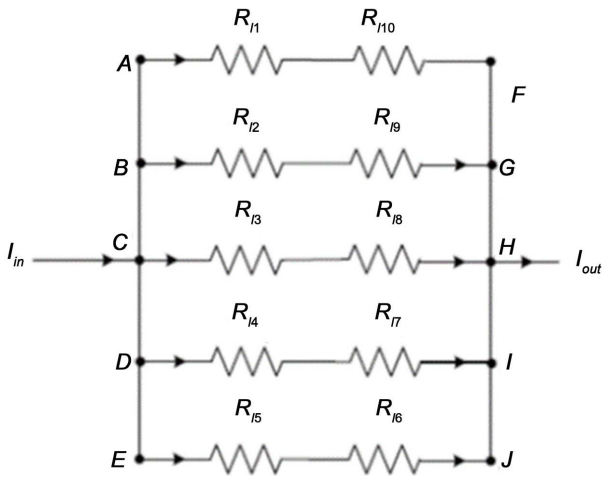

Figure 2. Semi series semi parallel wiring arrangement diagram.

Table 5. Total resistances values.

Connection mode	Total resistance @ 20˚C	Total resistance @ 150˚C
Series	56.266 Ω	89.143 Ω
Semi series/semi parallel	2.251 Ω	3.566 Ω

Table 6. Theoretical data for each coil.

Connection mode	Current in each layer (A)	Total Current (A)	Voltage (v)	Power (w)
Semi series/semi parallel	2.2882	11.4408	40.8	466.8

resistances are consistently higher than the calculated values; this is because each layer should be 800 turns which practically might be more than that.

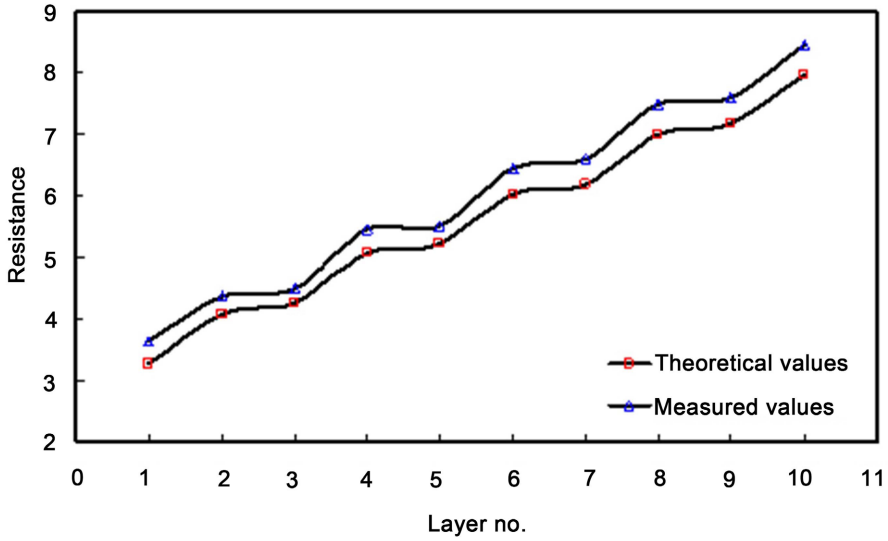

Figure 3. Comparison between theoretical and measured resistances of each layer.

The three coils are linked in series to collectively generate the necessary magnetic field strength, with the expectation that each individual coil contributes a magnetic field strength of 3000 Oersteds.

It's important to note that the resistivity of copper increases as temperature rises. To account for this temperature-related variation, a correction can be applied using the following relationship, especially for moderate temperature differences:

$$\rho = \rho_{r.t.}\left[1+\alpha\left(T-T_{r.t.}\right)\right] \tag{14}$$

where: T is the temperature in centigrade, and the subscripts *rt.* indicate a reference temperature

$$\rho_{r.t.} = 1.78\times10^{-8}\ \Omega\text{m}$$

$T_{r.t.}$ = 20˚C = reference temperature.

α = 0.00381˚C^{-1} = temperature coefficient of resistance of copper at 20˚C.

The apparatus is designed to have a maximum working temperature of about 150˚C; the resistivity at that temperature can be calculated using Equation (14):

$$\rho = 1.78\times10^{-8}\left[1+0.00381\left(150-20\right)\right] = 2.661634\times10^{-8}\ \Omega\text{m} \tag{15}$$

Figure 4 reveals the changes in resistance of each layer due to the maximum change in temperature.

2.5. The Cooling System and the Controls Associated with It

To minimize the heat generated in each coil, it was necessary to use an air cooling system which consisted of layers of copper tubes with outside diameters of 3 mm inserted between every two layers of windings as depicted in **Figure 5**. Compressed air is forced through the tubes at a pressure of 4 bars.

Within each coil, it is possible to place two temperature probes of the thermocouple type K. One probe is positioned between the first and second layers of

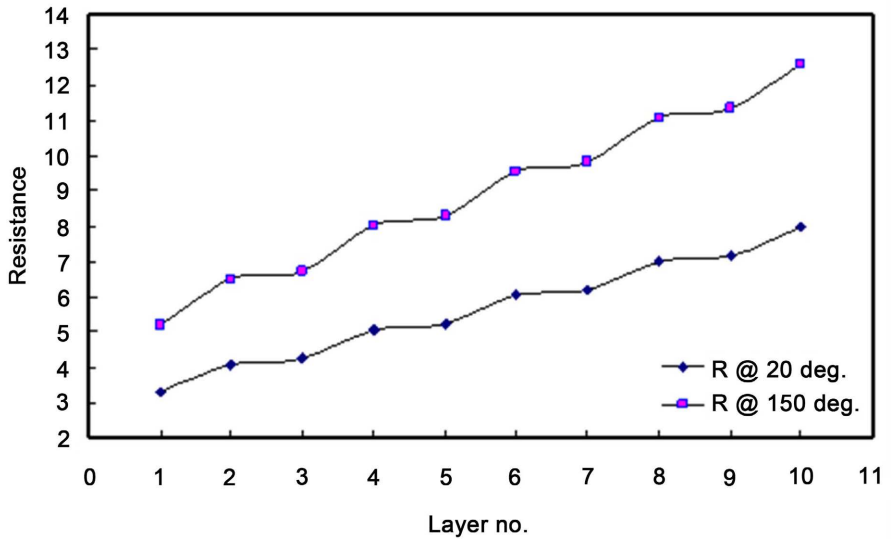

Figure 4. Changes in resistances due to changes in temperature.

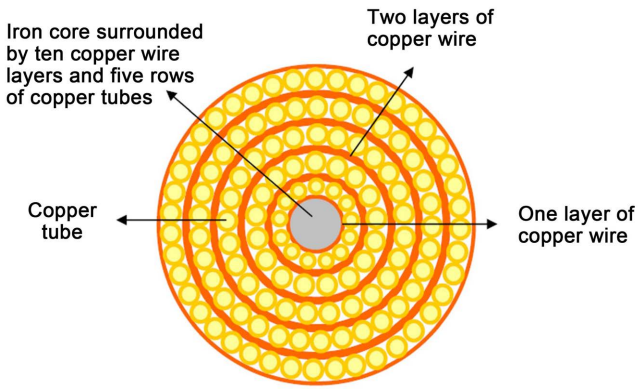

Figure 5. Distribution of copper tubes.

windings, while the other is located between the fifth and sixth layers. These probes serve to continually monitor temperature increases resulting from the heating of each coil.

To facilitate temperature monitoring and control, the temperature probes can be connected to an NI PCI_6024E data acquisition card (DAQ), which is integrated with LabVIEW software. This DAQ card has the capability to regulate the current supplied to the coil as well. All six thermocouples from the three coils can be connected to this single DAQ card, streamlining the data acquisition and control process.

2.6. Simulation Results

An analysis of the magnetic behavior of the apparatus was conducted using the Finite Element Method Magnetics (FEMM) software [9]. This specialized program is designed for solving electromagnetic problems within two-dimensional planar and axisymmetric domains. It has been widely adopted by researchers for simulating and analyzing magnetic field-related issues and has consistently

demonstrated reliable results [10] [11] [12].

In the simulation, the magnetic properties of non-magnetic materials such as air and copper were assumed to exhibit linearity, with a relative permeability of unity. For magnetic materials like low carbon steel, their behavior was assumed to follow the B-H curves provided within the software package. The simulation also included the same cobalt ferrite sample, with magnetic properties specified in **Table 3**.

The detailed characteristics of the three coils were input into the FEMM software package, and a current of 2.2882 Amps was applied to each layer within each coil. **Figure 6** depicts the distribution of magnetic flux along the iron core as computed in the simulation.

As **Figure 7** illustrates, the magnetic field intensity at the center of the air gap reaches approximately 14,177 Oersteds (1128.17 kA/m), with a minimum value of 1119.5 kA/m and an average of 1124 kA/m. It's worth noting that these values are slightly lower than the intensity predicted using Equation (6), which calculates it to be 1322.75 kA/m. The reason for this discrepancy is evident. The derivation of Equation (6) assumes a uniform magnetic flux throughout the entire C-shaped structure, including its "jaws." However, a glance at **Figure 6** reveals that this assumption isn't entirely accurate. There is some flux leakage occurring at various points in the circuit.

Leakage is observed at the corners of the iron core, but the most significant leakage occurs across the two ends of the C-shaped structure, where magnetic flux lines appear to bypass the sample. Estimating the extent of this flux leakage from the diagram is challenging, as the depiction tends to exaggerate it, making it difficult to gauge the amount of concentrated flux following the iron core. Consequently, it's not surprising that the more detailed and realistic Finite Element Method Magnetics (FEMM) simulation predicts a magnetic field strength at the air gap nearly 15% below the prediction based on Equation (6), which assumes ideal conditions with no flux leakage.

Due to this discrepancy between the FEMM predictions and the Equation (6) prediction, it is anticipated that the equipment will not attain the required 9000 Oersteds of magnetic field strength in the sample. Instead, the actual value is expected to be approximately 15% lower. However, there is a straightforward solution to correct this outcome—increasing the current by the same 15%, raising it from 2.2882 Amps to 2.63 Amps. This adjustment is expected to bring the equipment back in line with the original specifications. While it will generate additional heat, preliminary assessments suggest that the cooling system will effectively maintain the copper wiring well below the critical temperature of 150˚C.

3. Conclusions

A novel apparatus has been recently developed, offering the capability to investigate and analyse various magnetic properties, including magnetic annealing and

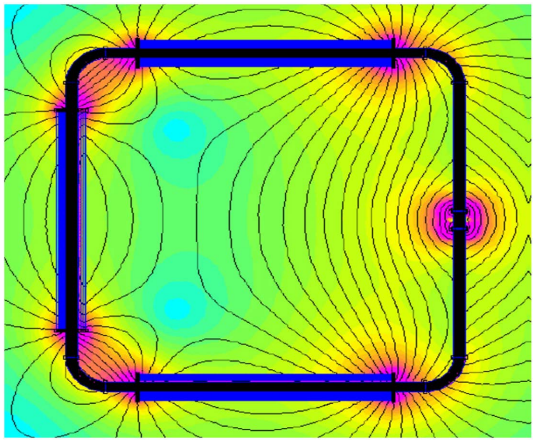

Figure 6. Magnetic flux distribution.

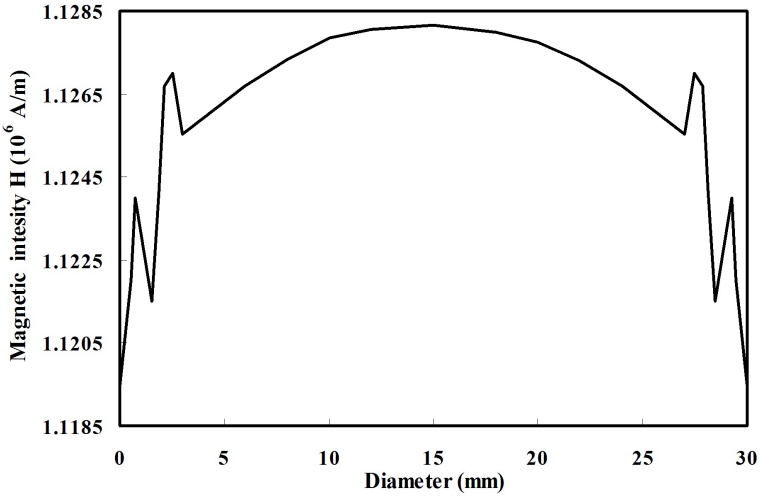

Figure 7. Magnitude of H along a diameter of the disc-shaped on either side of the sample.

its impact on magnetostriction, as well as the measurement of this property. This system successfully generated a robust and unchanging magnetic field strength of up to 9000 Oersted's.

The validity of the design was confirmed by comparing the anticipated outcomes obtained through the Finite Element Method Magnetics (FEMM) software package with the results calculated through other means. Fortunately, both sets of results exhibited a high degree of agreement and alignment.

Conflicts of Interest

The authors declare no conflicts of interest regarding the publication of this paper.

References

[1] Bitter, F. (1961) New Developments in High-Magnetic Field Research. *Physics Today*, **14**, 22-28. https://doi.org/10.1063/1.3057729

[2] Rafferty, A., Bakir, S., Brabazon, D. and Prescott, T. (2009) Calibration and Characterisation with a New Laser-Based Magnetostriction Measurement System. *Materials & Design*, **30**, 1680-1684. https://doi.org/10.1016/j.matdes.2008.07.026

[3] Jana, S. and Mukherjee, R.K. (2000) Generation and Measurement of Pulsed High Magnetic Field. *Journal of Magnetism and Magnetic Materials*, **214**, 234-242. https://doi.org/10.1016/S0304-8853(00)00194-3

[4] Ozaki, O., Koyanagi, K., Kiyoshi, T., Matsumoto, S., Fujihira, J. and Wada, H. (2002) Development of Superconducting Magnets for Uniform and High Magnetic Force Field Generation. *IEEE Transactions on Applied Superconductivity*, **12**, 940-943. https://doi.org/10.1109/TASC.2002.1018554

[5] Lo, C.C.H., Ring, A.P., Snyder, J.E. and Jiles, D.C. (2005) Improvement of Magnetomechanical Properties of Cobalt Ferrite by Magnetic Annealing. *IEEE Transactions on Magnetics*, **41**, 3676-3678. https://doi.org/10.1109/TMAG.2005.854790

[6] Kepuska, V.Z. and Elharati, H.A (2015) Performance Evaluation of Conventional and Hybrid Feature Extractions Using Multivariate HMM Classifier. *International Journal of Engineering Research and Applications* (*IJERA*), **5**, 96-101.

[7] Bozorth, R.M., Tilden, E.F. and Williams, A.J. (1955) Anisotropy and Magnetostriction of Some Ferrites. *Physical Review Journals Archive*, **99**, 1788-1798. https://doi.org/10.1103/PhysRev.99.1788

[8] Ryff, P.F. (1994) Electric Machinery. 2nd Edition, Prentice Hall Inc., Hoboken.

[9] Hammond, P. (1986) Electromagnetism for Engineers. 3rd Edition, Pergamon Press, Oxford.

[10] (2007) Meeker DC, "FEMM". http://femm.foster-miller.net

[11] Grossinger, R., Küpferling, M., Kasperkovitz, P., *et al.* (2002) Eddy Currents in Pulsed Field Measurements. *Journal of Magnetism and Magnetic Materials*, **242-245**, 911-914. https://doi.org/10.1016/S0304-8853(01)01324-5

[12] Marghani, K., Elhaj, A., Sims, A. and Elharati, H. (2023) Fractal Analysis on the Detection of the Malignancy Changes of Pancreatic Cancer. *The Libyan Journal of Science*, **236**, 24-32.